J|A|C|S
ARTICLES
Published on Web 05/23/2002

$TpPtMe(H)_2$: Why Is There H/D Scrambling of the Methyl Group but Not Methane Loss?

Mark A. Iron,[†] H. Christine Lo,[‡] Jan M. L. Martin,*[,†] and Ehud Keinan*[,‡,§]

Contribution from the Department of Organic Chemistry, Weizmann Institute of Science, 76100 Rehovot, Israel, Scripps Research Institute, 10550 North Torrey Pines Road, La Jolla, California 92037, and Department of Chemistry, Technion - Israel Institute of Technology, 32000 Haifa, Israel

Received January 22, 2002

Abstract: The reactivity of $TpPtMe(H)_2$ (Tp = hydrido-tris(pyrazolyl)borate) was investigated. This complex is remarkably resistant to methane loss; heating it in methanol at 55 °C does not lead to either methane or hydrogen loss. When CD_3OD is used, reversible H/D scrambling of the hydrides and the methyl hydrogens occurs. This reactivity was investigated by density functional theory (DFT) methods at the mPW1k/LANL2DZ+P//mPW1k/LANL2DZ level. It was found that methane loss cannot occur due to the rigidity of the Tp ligand, which does not allow the *trans* geometry which would be required for the product of methane elimination, TpPtH. The resulting complex is very high in energy, and therefore the loss of methane is unfavorable. On the other hand, H/D scrambling of the methyl ligand is relatively facile. It proceeds through an η^{2-CH}-CH_4 complex, even though methane loss is not observed. The model system, $[(NH_3)_3PtMe(H)_2]^+$ was examined to verify that the cause of the observations is the rigidity of the Tp system. The reaction was investigated at a number of levels of DFT. It was concluded that investigations of similar sized systems should be examined at the above level of theory or the mPW1k/SDB-cc-pVDZ//mPW1k/SDD level for improved accuracy of the energetic calculations.

Introduction

Although alkanes have been reported to oxidatively add to several transition-metal complexes (for recent reviews, see refs 1−12), the practical and selective metal-catalyzed functionalization of an alkane remains a formidable challenge.[13−18] Of the transition-metal complexes that were found to be capable of C−H activation, those of platinum[19,20] have drawn substantial attention, especially the Shilov system[13,21] and the Pt(II)-catalyzed oxidation of methane observed by Periana et al.[14,15] A few electronically and coordinatively unsaturated Pt(II) complexes were found to add inactive C−H bonds. Such reactive complexes were generated from their Pt(II)-dimethyl precursors either by the addition of an acid to eliminate CH_4[22−24] or a strong electrophilic reagent to abstract a methyl anion.[25] Clearly, the development of useful C−H activation strategies relies heavily on the thorough understanding of the parameters governing the mechanism, reactivity and selectivity of these reactions. Indeed, significant efforts have been invested to gain mechanistic understanding to establish a tuneable alkane functionalization system.[1−12]

An important conceptual advance in the field has been the proposed existence of a σ-alkane complex in both the oxidative addition and the reductive elimination pathways.[26−31] It has also

* Author e-mail addresses: comartin@wicc.weizmann.ac.il, keinan@scripps.edu.
[†] Weizmann Institute of Science.
[‡] Scripps Research Institute.
[§] Technion - Israel Institute of Technology.

(1) Parshall, G. W. *Acc. Chem. Res.* **1975**, *8*, 113.
(2) Parshall, G. W. *Catalysis* **1977**, *1*, 335.
(3) Muetterties, E. L. *Chem. Soc. Rev.* **1982**, *11*, 283.
(4) Shilov, A. E. *Activation of Saturated Hydrocarbons by Transition Metal Complexes*; Riedel: Dordrecht, 1984.
(5) Hill, C. L. In *Activation and Functionalization of Alkanes*; Hill, C. L., Ed.; Wiley: New York, 1989.
(6) Lee, A. J.; Purwoko, A. A. *Coord. Chem. Rev.* **1994**, *132*, 155.
(7) Arndtsen, B. A.; Bergman, R. G.; Mobley, T. A.; Petersson, T. H. *Acc. Chem. Res.* **1995**, *28*, 154.
(8) Sen, A. In *New Approaches in C-H Activation of Alkanes in Applied Homogeneous Catalysis with Organometallic Compounds: A Comprehensive Handbook in Two Volumes*; Cornil, B., Herrman, W. A., Eds.; Wiley-VCH: New York, 1996.
(9) Shilov, A. E.; Shul'pin, G. B. *Chem. Rev.* **1997**, *97*, 2879.
(10) Stahl, S. S.; Labinger, J. A.; Bercaw, J. E. *Angew. Chem., Int. Ed.* **1998**, *37*, 2180.
(11) Shilov, A. E.; Shul'pin, G. B. *Activation and Catalytic Reactions of Saturated Hydrocarbons in the Presence of Metal Complexes*; Kluwer: Dordrecht, 2000.
(12) Crabtree, R. H. *J. Chem. Soc., Dalton Trans.* **2001**, 2437.
(13) Goldshleger, N. F.; Eskova, V. V.; Shilov, A. E.; Shteinman, A. A. *Zh. Fiz. Khim.* **1972**, *46*, 1353.
(14) Periana, R. A.; Taube, D. J.; Gamble, S.; Taube, H.; Satoh, T.; Fujii, H. *Science* **1998**, *280*, 560.
(15) Kua, J.; Xu, X.; Periana, R. A.; Goddard, W. A., III. *Organometallics* **2002**, *21*, 511.
(16) Waltz, K. M.; Hartwig, J. F. *Science* **1997**, *277*.
(17) Waltz, K. M.; Hartwig, J. F. *J. Am. Chem. Soc.* **2000**, *122*, 11358.
(18) Chepaikin, E. G.; Bezruchenko, A. P.; Leshcheva, A. A.; Boyko, G. N.; Kuzmenkov, I. V.; Grigoryan, E. H.; Shilov, A. E. *J. Mol. Catal. A: Chem.* **2001**, *169*, 89.
(19) Anderson, G. K. In *Comprehensive Organometallic Chemistry*, 2nd ed.; Puddephatt, R. J., Ed.; Pergamon: Oxford, UK, 1995; Vol. 9, Chapter 9 and references therein.
(20) Puddephatt, R. J. *Coord. Chem. Rev.* **2001**, *219*−*221*, 157.
(21) Siegbahn, P. E. M.; Crabtree, R. H. *J. Am. Chem. Soc.* **1996**, *118*, 4442.
(22) Holtcamp, M. W.; Labinger, J. A.; Bercaw, J. E. *J. Am. Chem. Soc.* **1997**, *119*, 848.
(23) Johansson, L.; Tilset, M.; Labinger, J. A.; Bercaw, J. E. *J. Am. Chem. Soc.* **2000**, *122*, 10846.
(24) Johansson, L.; Ryan, O. B.; Tilset, M. *J. Am. Chem. Soc.* **1999**, *121*, 1974.
(25) Wick, D. D.; Goldberg, K. I. *J. Am. Chem. Soc.* **1997**, *119*, 10235.

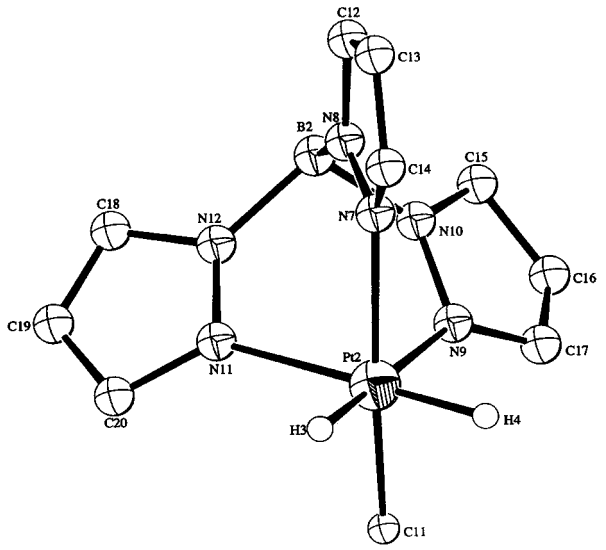

Figure 1. X-ray crystal structure of **1**. The platinum hydride ligands were placed in their calculated postions. See Experiemental Section for further details.

been proposed that strong metal-to-alkane π-back-bonding would enhance metal−alkane binding, and yet, when the back-bonding becomes very strong, the C−H bond would oxidatively add to the metal.[28,32] Obviously, the availability of either a thermally or kinetically stable σ-alkane complex would offer attractive opportunities to study the nature of alkane activation and functionalization. Although convincing evidence for the existence of σ-alkane complexes has been provided by modern techniques, such as low-temperature NMR spectroscopy,[33,34] ultrafast IR,[35,36] and gas-matrix isolation with UV−vis characterization,[37] the experimental characterization of a σ-alkane complex is still an overwhelming challenge. Nevertheless, in one notable work, an iron−heptane complex was characterized by X-ray crystallography.[38]

In 1999, we reported on an air- and moisture-stable alkyldihydrido platinum(IV) complex, $TpPtMe(H)_2$ (**1**, Tp = hydridotris(pyrazolyl)borate) (Figure 1). The use of the Tp and similar ligands has grown in popularity in recent years.[39−46]

Scheme 1

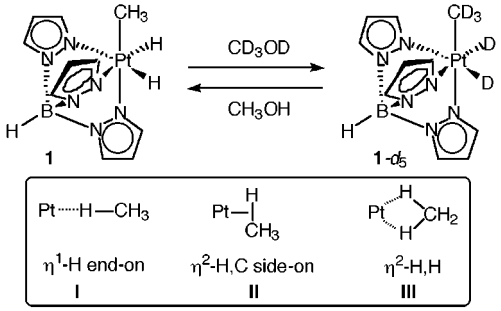

Compound **1** was prepared from TpPt(II)Me(CO) and water at room temperature[47] via a mechanistic pathway that probably involves water attack on the carbonyl ligand, in analogy to the water−gas shift (WGS) reaction, and direct protonation on the metal, similar to the low-temperature oxidation of Pt(II) to Pt(IV) with HCl[48−51] or with HBF_4.[52] The thermal stability of **1** was believed to be attributed to the special properties of the tridentate Tp ligand. In a recent preliminary communication,[32] we reported that the methyl hydrogens in **1** undergo H/D exchange in methanol at 55 °C. The H/D exchange indicates that under these conditions complex **1** coexists in a fast equilibrium with $TpPt(II)H(\sigma\text{-}CH_4)$, which is kinetically inert to liberation of methane (Scheme 1). To the best of our knowledge, this is the first example of a hydridoalkylmetal complex that undergoes isotopic scrambling at elevated temperatures without concomitant liberation of either alkane or dihydrogen.

Herein we present our combined experimental and theoretical investigation into the reactivity of complex **1**. In particular, we try to understand why the σ-CH_4 ligand in $TpPt(II)H(\sigma\text{-}CH_4)$ is "sticky" and is not liberated from the platinum complex. To answer this question we compared the reactivity of **1** with that of the model tris-monodentate *fac*-$[(NH_3)_3PtMe(H)_2]^+$ system by means of density functional theory (DFT).

Experimental Section

General Methods. Unless otherwise specified, NMR spectra were recorded at room temperature on either a Bruker AMX-400, DRX-500, or a DRX-600 MHz spectrometer. The ^{1}H NMR signals are reported in ppm downfield from tetramethylsilane and referenced to residual solvent resonances (^{1}H NMR: 5.32 for $CDHCl_2$, 7.24 for $CHCl_3$). The chemical shift values are given in ppm followed by multiplicity, coupling constants, *J*, in Hertz, and relative integration. Assignments are provided for key moieties only. The $^{31}P\{^1H\}$ NMR chemical shifts are referenced to 85% H_3PO_4 (aq) as an external standard. J. Young NMR tubes, featuring a resealable Teflon threaded cap, were pre-silylated with 1,1,1,3,3,3-hexamethyldisilazane to avoid acid-catalyzed hydrophilic reactions. Unless otherwise noted, all reactions and manipulations were conducted under an argon atmosphere in a Vacuum Atmospheres glovebox or by using Schlenk techniques.

(26) Periana, R. A.; Bergman, R. G. *J. Am. Chem. Soc.* **1986**, *108*, 7332.
(27) Mobley, T. A.; Schade, C.; Bergman, R. G. *Organometallics* **1998**, *17*, 3574.
(28) Hall, C.; Perutz, R. N. *Chem. Rev.* **1996**, *96*, 3125.
(29) Grigoryan, E. H. *Kinet. Catal.* **1999**, *40*, 350.
(30) For nonsolvent involved reactions, it is also possible that a net inverse isotope effect on the rate of H/D scrambling could be accommodated by two normal isotope effects with the forward reaction (the reductive coupling step) being smaller and the reverse reaction (the oxidative addition step) being larger; for an example, see: Wick, D. D.; Reynolds, K. A.; Jones, W. D. *J. Am. Chem. Soc.* **1999**, *121*, 3974.
(31) Northcutt, T. O.; Wick, D. D.; Vetter, A. J.; Jones, W. D. *J. Am. Chem. Soc.* **2001**, *123*, 7257.
(32) Lo, H. C.; Haskel, A.; Kapon, M.; Keinan, E. *J. Am. Chem. Soc.* **2002**, *124*, 3226.
(33) Geftakis, S.; Ball, G. E. *J. Am. Chem. Soc.* **1998**, *120*, 9953.
(34) Garel, L.; Dutasta, J.-P.; Collet, A. *Angew. Chem., Int. Ed. Engl.* **1993**, *32*, 1169.
(35) Schultz, R. H.; Bengali, A. A.; Tauber, M. J.; Weiller, B. H.; Wasserman, E. P.; Kyle, K. R.; Moore, C. B.; Bergman, R. G. *J. Am. Chem. Soc.* **1994**, *116*, 7369.
(36) Sun, X. Z.; Grills, D. C.; Nikiforov, S.; Poliakoff, M.; George, M. W. *J. Am. Chem. Soc.* **1997**, *119*, 7521.
(37) Perutz, R. N.; Turner, J. J. *J. Am. Chem. Soc.* **1975**, *97*, 4791.
(38) Evans, D. R.; Drovetskaya, T.; Bau, R.; Reed, C. A.; Boyd, P. D. W. *J. Am. Chem. Soc.* **1997**, *119*, 3633.
(39) Slugovc, C.; Schmid, R.; Kirchner, K. *Coord. Chem. Rev.* **1999**, *186*, 109.
(40) Vahrenkamp, H. *Acc. Chem. Res.* **1999**, *32*, 589.
(41) Trofimenko, S. *Scorpionates: The Coordination Chemistry of Polypyrazolylborate Ligands*; Imperial College Press: London, 1999.
(42) Reger, D. L. *Coord. Chem. Rev.* **1996**, *96*, 571.
(43) Parkin, G. *Adv. Inorg. Chem.* **1995**, *42*, 291.
(44) Kitajima, N.; Tolman, B. W. *Prog. Inorg. Chem.* **1995**, *43*, 419.
(45) Trofimenko, S. *Chem. Rev.* **1993**, *93*, 943.
(46) Tellers, D. M.; Skoog, S. J.; Bergman, R. G.; Gunnoe, T. B.; Harman, W. D. *Organometallics* **2000**, *19*, 2428.
(47) Haskel, A.; Keinan, E. *Organometallics* **1999**, *18*, 4677.
(48) Stahl, S. S.; Labinger, J. A.; Bercaw, J. E. *J. Am. Chem. Soc.* **1995**, *117*, 9371.
(49) Hill, G. S.; Rendina, L. M.; Puddephatt, R. J. *Organometallics* **1995**, *14*, 4966.
(50) De Felice, V.; De Renzi, A.; Panuzi, A.; Tesauro, D. *J. Organomet. Chem.* **1995**, *488*, C13.
(51) O'Reilly, S. A.; White, P. S.; Templeton, J. L. *J. Am. Chem. Soc.* **1996**, *118*, 5684.
(52) Canty, A. J.; Dedieu, A.; Jin, H.; Milet, A.; Richmond, M. K. *Organometallics* **1996**, *15*, 2845.

General Procedure for Kinetic Experiments. In a typical experiment, a presilylated J. Young NMR tube was charged with **1** and an internal standard ($(Me_3Si)_4C$), and Schlenk techniques were used to deoxygenate the solid mixture. The deuterated solvent (0.8 mL, dried over powdered 4Å molecular sieves for at least 24 h) was added under argon, and the resulting solution was further deoxygenated by three freeze−pump−thaw cycles. The resulting sample was then stored at −78 °C before being placed into the NMR probe at 55 °C. The progress of the reaction was recorded on a DRX-600 NMR spectrometer with a built-in kinetic software, and the acquisition parameters for each spectrum were as follows: NS = 1, 90° pulse, $D_1 > 5T_1 - AT$, interval = 5 min, where: NS = number of transient, D_1 = delay time, T_1 = relaxation time, AT = acquisition time.

X-ray Crystallography. A colorless thin plate of complex **1** was mounted on the Nonius Kappa CCD diffractometer with the ϕ axis almost parallel to the plate plane. Accurate cell parameters were obtained from 56367 reflections using Mo Kα radiation. Data collection was performed with ϕ scans and ω scans to fill in the Ewald Sphere. The crystal-to-detector distance was increased to 6.0 cm to improve resolution between diffraction spots. Numerical absorption corrections were applied to the intensities after the crystal shape was accurately defined.

The complex Pt atomic positions were located by direct methods and the light atoms by successive Fourier difference maps. The structure was refined anisotropically for the Pt atoms and isotropically for the light atoms, but refinement at this stage gave very unsatisfactory discrepancy factor $R = 0.176$. Residual electron densities were totally meaningless, regarding any additional chemical moieties, but molecular packing was found quite reasonable. After some effort, a twinning model was suggested on the basis of the proximity of the cell angle β to 90°. A twin law −1 0 0 0 1 0 0 0 1 was introduced into the least-squares routine, and after four cycles, the *R* factor dropped from 0.176 to 0.073. Refinement gave a twin component of 0.277(3), indicating that the crystal is a composite of 78% of one component and 22% of a second component with its *a* axis reversed. Here, the twin model was found successful because splitting between spots from each of the components was rather small and allowed spot integration of both contributions. Residual electron density of 3.78 e/Å^3 found around the Pt atom was attributed to absorption effect. No attempt was made at this stage to introduce hydrogens at calculated positions including those two attached to the Pt atom that complete the octahedral coordination sphere. Full details can be found in the Supporting Information.

Several programs were used for data processing and refinement. The data collection used Kappa CCD Server software.[53] The cell refinement and data reduction made use of DENZO-SMN.[54] The structure solution and refinement utilized the SHELXL-97 program.[55] This same program was used to prepare the material for publication. Molecular graphics involved the structure analysis package, TEXSAN 1.6f.[56]

Computational Details. All calculations were carried out using *Gaussian 98*, Revision A7[57] running on Compaq ES40 and XP1000 workstations in our group, on an experimental Linux PC Farm at the Faculty of Physics, and on the SGI Origin computers of the Faculty of Chemistry and the (Israel) Inter-University Computing Center. The patch to *Gaussian 98* as detailed in the Appendix to ref 58 was applied.

Two exchange-correlation functionals were considered. The first is the highly popular B3LYP (Becke 3-parameter exchange[59,60] with Lee−Yang−Parr correlation[61]) functional. The second is the very recent mPW1k (modified Perdew−Wang 1-parameter for kinetics) functional of Truhlar and co-workers.[62] It has been shown (e.g., refs 62−64) that this functional generally yields much more reliable reaction barrier heights than B3LYP or other "conventional" exchange-correlation functionals.

Five basis set-RECP (relativistic effective core potential) combinations were considered. The first is the standard Hay−Wadt LANL2DZ (Los Alamos National Laboratory Double-ζ) combination[65] on transition metals, combined with the Dunning−Hay[66] valence double-ζ basis set on the lighter elements. The second, denoted LANL2DZ+P, combines the Dunning−Hay valence double-ζ plus polarization basis set on the lighter elements with LANL2DZ on the transition metals, supplemented by *f*-type polarization functions taken from the work of Frenking and co-workers.[67,68] The third, denoted SDD, is the combination of the Huzinaga−Dunning double-ζ basis set on lighter elements with the Stuttgart−Dresden basis set-RECP combination[69] on the transition metals. The fourth, SDB-cc-pVDZ, combines the Dunning cc-pVDZ basis set[70] on the main group elements with the Stuttgart−Dresden basis set−RECP combination[69] on the transition metals, with an *f*-type polarization exponent taken as the geometric average of the two *f*-exponents given in the Appendix to ref 71. The fifth is SDB-cc-pVTZ. This combines the Dunning cc-pVTZ basis set[70] on the main group elements with Stuttgart−Dresden on the transition metals, with the two *f*-type and one *g*-type polarization exponents given in the Appendix to ref 71. For interpretative purposes, Wiberg bond indices[72] were derived from the natural bond order (NBO) analysis[73] at the mPW1k/LANL2DZ level.

Experimental Results and Discussion

The thermal stability of **1** was evident from the fact that no spectral change could be observed even after heating at 55−70 °C in CH_3OH for several hours. However, when **1** was heated at the same temperatures in either CD_3OD or in a 1:1 mixture of C_6H_6 and CD_3OD, the hydride and methyl signals disappeared completely from the ^{1}H NMR spectrum with no change in the Tp signals. Remarkably, when the resultant **1**-d_5 was heated under the same conditions in CD_3OH, it was quantitatively converted back to **1** (Scheme 1). Clearly, liberation of methane, with or without C−H activation of benzene, does not occur under these conditions.

(53) Kappa CCD Server Software; Nonius, B. V.: Delft, The Netherlands, 1997.
(54) Otwinowski, Z.; Minor, W. *Methods Enzymol.* **1997**, *276*, 307.
(55) Sheldrick, G. M. Institut fur Anorganische Chemie, Universitat Göttingen: Göttingen, Germany, 1997.
(56) *TEXSAN*, 1.6f ed.; Molecular Structure Corp.: The Woodlands, TX, 1992.
(57) Frisch, M. J.; Trucks, G. W.; Schlegel, H. B.; Scuseria, G. E.; Robb, M. A.; Cheeseman, J. R.; Zakrzewski, V. G.; Montgomery, J. A., Jr.; Stratmann, R. E.; Burant, J. C.; Dapprich, S.; Millam, J. M.; Daniels, A. D.; Kudin, K. N.; Strain, M. C.; Farkas, O.; Tomasi, J.; Barone, V.; Cossi, M.; Cammi, R.; Mennucci, B.; Pomelli, C.; Adamo, C.; Clifford, S.; Ochterski, J.; Petersson, G. A.; Ayala, P. Y.; Cui, Q.; Morokuma, K.; Malick, D. K.; Rabuck, A. D.; Raghavachari, K.; Foresman, J. B.; Cioslowski, J.; Ortiz, J. V.; Stefanov, B. B.; Liu, G.; Liashenko, A.; Piskorz, P.; Komaromi, I.; Gomperts, R.; Martin, R. L.; Fox, D. J.; Keith, T.; Al-Laham, M. A.; Peng, C. Y.; Nanayakkara, A.; Gonzalez, C.; Challacombe, M.; Gill, P. M. W.; Johnson, B. G.; Chen, W.; Wong, M. W.; Andres, J. L.; Head-Gordon, M.; Replogle, E. S.; Pople, J. A. *Gaussian 98*, revision A.7; Gaussian, Inc.: Pittsburgh, PA, 1998.
(58) Martin, J. M. L.; Bauschlicher, C. W.; Ricca, A. *Comput. Phys. Commun.* **2001**, *133*, 189.
(59) Becke, A. D. *J. Chem. Phys.* **1993**, *98*, 5648.
(60) Stevens, P. J.; Devlin, F. J.; Chabalowski, C. F.; Frisch, M. J. *J. Phys. Chem.* **1994**, *98*, 11623.
(61) Lee, C.; Yang, W.; Parr, R. G. *Phys. Rev. B* **1988**, *38*, 3098.
(62) Lynch, B. J.; Fast, P. L.; Harris, M.; Truhlar, D. G. *J. Phys. Chem. A* **2000**, *104*, 4811.
(63) Lynch, B. J.; Truhlar, D. G. *J. Phys. Chem. A* **2001**, *105*, 2936.
(64) Parthiban, S.; de Oliveira, G.; Martin, J. M. L. *J. Phys. Chem. A* **2001**, *105*, 895.
(65) Hay, P. J.; Wadt, W. R. *J. Chem. Phys.* **1985**, *82*, 299.
(66) Dunning, T. H., Jr.; Hay, P. J. In *Modern Theoretical Chemistry*; Schaefer, H. F., III, Ed.; Plenum Press: New York NY, 1977; Vol. 4.
(67) Ehlers, A. W.; Bohme, M.; Dapprich, S.; Gobbi, A.; Hollwarth, A.; Jonas, V.; Kohler, K. F.; Stegmann, R.; Veldkamp, A.; Frenking, G. *Chem. Phys. Lett.* **1993**, *208*, 111.
(68) Hollwarth, A.; Bohme, M.; Dapprich, S.; Ehlers, A. W.; Gobbi, A.; Jonas, V.; Kohler, K. F.; Stegmann, R.; Veldkamp, A.; Frenking, G. *Chem. Phys. Lett.* **1993**, *208*, 237.
(69) Dolg, M. In *Modern Methods and Algorithms of Quantum Chemistry*; Grotendorst, J., Ed.; John von Neumann Institute for Computing: Jülich, 2000; Vol. 1, pp 479−508.
(70) Dunning, T. H., Jr. *J. Chem. Phys.* **1989**, *90*, 1007.
(71) Martin, J. M. L.; Sundermann, A. *J. Chem. Phys.* **2001**, *114*, 3408.
(72) Wiberg, K. B. *Tetrahedron* **1968**, *24*, 1083.
(73) Reed, A. E.; Curtiss, L. A.; Weinhold, F. *Chem. Rev.* **1988**, *88*, 899.

Since the observed H/D exchange suggests the existence of a σ-alkane intermediate, the rates of this exchange were further pursued. A solution of **1** in CD_3OD (0.8 mL) was heated in an NMR probe at 55 °C, and the progress of the reaction was monitored by ^1H NMR for 6 h until both the hydride ($\delta = -19.85$ ppm) and methyl ($\delta = 1.06$ ppm) signals could no longer be detected. Since the time for the disappearance of the hydride signal (less than 5 min) was much shorter than that of the methyl signal (several hours), we considered the H/D exchange between hydride ligands and solvent molecules as a fast preequilibrium step and neglected its contribution to the kinetic isotope effect. After the reaction ran to completion, the solvent was carefully removed under high vacuum, CD_3OH (0.8 mL) was added, and the resulting solution of **1**-d_5 was heated in the NMR probe as described above. Pseudo-first-order kinetics were observed in both the conversion of **1** to **1**-d_5 ($k_{obs}^D = 2.42(3) \times 10^{-4}$ s^{-1}, $t_{1/2} \approx 48$ min), and the reversion of **1**-d_5 to **1** ($k_{obs}^H = 1.84(5) \times 10^{-4}$ s^{-1}, $t_{1/2} \approx 63$ min). From this, one obtains a kinetic isotope effect of $k_H/k_D = 0.76$.

An inverse kinetic isotope effect can occur in a reaction that is characterized by a single rate-determining step with a product-like transition state.[74,75] For the reductive coupling in hydridoalkyl−metal complexes, the inverse kinetic isotope effect could stem from the fact that the energy barrier for breaking a deuterium−metal bond is lower than that of a proton−metal bond. Such effects were previously observed for the loss of alkanes from hydridoalkyl complexes via a proposed σ-alkane intermediate (k_H/k_D ranging from 0.29 to 0.80).[26,30,31,76−81] The isotope effects in these reports were obtained by measuring the relative rates of alkane liberation. By contrast, liberation of methane could not be detected in our case. We therefore propose that our observed inverse kinetic isotope effect ($k_H/k_D = 0.76$) should reflect the $\Delta G^‡$ of the reductive coupling step, in which a σ-methane Pt(II) complex is formed, but not the $\Delta G^‡$ of the overall process, in which a dealkylated Pt(II) complex and free methane are formed. Accordingly, this demonstrates that the conversion of **1** to the σ-methane Pt(II) complex, **2**, has a lower barrier than the conversion of **2** to the dealkylated Pt(II) complex, **4**, and free methane. In the previous reports on σ-alkanes, the barriers for the transition from **2** to **4** appeared to be either lower or comparable to that of the transition from **1** to **2**.[82]

There are several experimental observations[31,33,83,84] and theoretical calculations[21,85−91] that can support such a mechanism. An alternative route to H/D scrambling involves α-H elimination. While this is rare, there are examples of this route.[92,93]

Theoretical Results and Discussion

The application of computational methods to problems in organometallic chemistry has been increasing dramatically in recent years as a result of improvements in methodology and computing power.[94] We have employed DFT calculations to investigate various systems, including the rhodium-catalyzed C−H and C−C bond activation using PCP,[95] PCN,[96] and PCO[97] systems, the palladium-catalyzed Heck reaction[98] and the stabilization of silanones.[99,100] In the present study, we have employed the recent mPW1k hybrid exchange-correlation functional developed by Truhlar and co-workers.[62] This functional has been shown (e.g., refs 62−64) to yield more accurate reaction barrier heights than other functionals, including the very popular B3LYP. In addition, basis set convergence is considered in some detail. On the basis of the results obtained, we can conclude that the popular B3LYP/LANL2DZ exchange-correlation functional-basis set combination is insufficient for investigating reactions and can lead to erroneous conclusions. Instead we recommend using the mPW1k functional in conjunction with a basis set of at least double-ζ plus polarization quality, such as the combination conventionally denoted mPW1k/SDB-cc-pVDZ//mPW1k/SDD.

The initial investigation was performed at the mPW1k/LANL2DZ level. The geometries reported herein are all at this level of theory unless indicated otherwise. To further improve the accuracy of the calculated reaction profile, single-point energies at these reference geometries were calculated at the mPW1k/LANL2DZ+P level. Unless otherwise noted, energies are at this mPW1k/LANL2DZ+P//mPW1k/LANL2DZ level. All energies reported are relative to the starting complex, $TpPtMe(H)_2$ (**1**), or $(NH_3)_3PtMe(H)_2$ (**9**) in the tris-ammonia case (vide infra), unless indicated otherwise. Table 1 lists the energies of the various complexes, and each complex will be discussed below.

Starting Complex. The starting complex is $TpPtMe(H)_2$ (**1**) and its computed structure is depicted in Figure 2 along with the other participants in the reductive elimination reaction. Complex **1** has an octahedral structure with C_s symmetry. As expected, the tridentate Tp ligand is bound in a facial (*fac*) geometry. The meridional (*mer*) geometry is impossible because

(74) Bigeleisen, J. *Pure Appl. Chem.* **1964**, *8*, 217.
(75) Halpern, J. *Pure Appl. Chem.* **1986**, *58*, 575.
(76) Buchanan, J. M.; Stryker, J. M.; Bergman, R. G. *J. Am. Chem. Soc.* **1986**, *108*, 1537.
(77) Stahl, S. S.; Labinger, J. A.; Bercaw, J. E. *J. Am. Chem. Soc.* **1996**, *118*, 5961.
(78) Wang, C.; Ziller, J. W.; Flood, T. C. *J. Am. Chem. Soc.* **1995**, *117*, 1647.
(79) Bullock, R. M.; Headford, C. E. L.; Hennessy, K. M.; Kegley, S. E.; Norton, J. R. *J. Am. Chem. Soc.* **1989**, *111*, 3897.
(80) Gould, G. L.; Heinekey, D. M. *J. Am. Chem. Soc.* **1989**, *111*, 5502.
(81) Parkin, G.; Bercaw, J. E. *Organometallics* **1989**, *8*, 1172.
(82) Most of the theoretical studies with Pt and Pd that compared the reductive coupling of H−H, H−C, and C−C have focused on the transition between d^8 and d^{10} configurations. Information about d^6-to-d^8 transition is relatively rare. It is commonly accepted that the activation barrier for the overall reductive elimination is sensitive to the nature of the bond being formed. The spherically symmetric orbital of hydrogen appears to allow it to simultaneously form H−H bonds while breaking M−H bonds, resulting in a smaller energy barrier relative to that of C−H coupling. See: Low, J. J.; Goddard, W. A., III. *J. Am. Chem. Soc.* **1984**, *106*, 8321. Therefore, we assume that the formation of a σ-H_2 complex would be a much faster process in comparison with the formation of a σ-CH_4 complex and its effect on the overall exchange rate can be neglected.
(83) Johansson, L.; Tilset, M. *J. Am. Chem. Soc.* **2001**, *123*, 739.
(84) Gross, C.; Girolami, G. S. *J. Am. Chem. Soc.* **1998**, *120*, 6605.
(85) Heiberg, H.; Swang, O.; Ryan, O. B.; Gropen, O. *J. Phys. Chem. A* **1999**, *103*, 10004.
(86) Bartlett, K. L.; Goldberg, K. I.; Borden, W. T. *J. Am. Chem. Soc.* **2000**, *122*, 1456.
(87) Strout, D. L.; Zarić, S.; Niu, S.; Hall, M. B. *J. Am. Chem. Soc.* **1996**, *118*, 6068.
(88) Su, M.-D.; Chu, S.-Y. *J. Am. Chem. Soc.* **1997**, *119*, 5373.
(89) Siegbahn, P. E. M. *J. Am. Chem. Soc.* **1996**, *118*, 1487.
(90) Gérard, H.; Eisenstein, O.; Lee, D.-H.; Chen, J.; Crabtree, R. H. *New J. Chem.* **2001**, *25*, 1121.
(91) Martin, R. L. *J. Am. Chem. Soc.* **1999**, *121*, 9459.
(92) Hayes, J. C.; Cooper, N. J. *J. Am. Chem. Soc.* **1982**, *104*, 5570.
(93) Bullock, R. M.; Headford, C. E. L.; Kegley, S. E.; Norton, J. R. *J. Am. Chem. Soc.* **1985**, *107*, 727.
(94) Niu, S.; Hall, M. B. *Chem. Rev.* **2000**, *100*, 353.
(95) Sundermann, A.; Uzan, O.; Milstein, D.; Martin, J. M. L. *J. Am. Chem. Soc.* **2000**, *122*, 7095.
(96) Sundermann, A.; Uzan, O.; Martin, J. M. L. *Organometallics* **2001**, *20*, 1703.
(97) Rybtchinski, B.; Oevers, S.; Montag, M.; Vigalok, A.; Rozenberg, H.; Martin, J. M. L.; Milstein, D. *J. Am. Chem. Soc.* **2001**, *123*, 9064.
(98) Sundermann, A.; Uzan, O.; Martin, J. M. L. *Chem. Eur. J.* **2001**, *7*, 1703.
(99) Uzan, O.; Martin, J. M. L. *Chem. Phys. Lett.* **1998**, *290*, 535.
(100) Uzan, O.; Gozin, Y.; Martin, J. M. L. *Chem. Phys. Lett.* **1998**, *288*, 356.

Table 1. Relative Energies (ΔG_{298}) at the mPW1k/LANL2DZ+P//mPW1k/LANL2DZ Level of the Various Complexes

complex	Tp system	NH_3 system
$N_3PtMe(H)_2$ (**1** or **9**)	0.0	0.0
$N_2PtMe(H)_2$ (**10**)	−	a) 25.0
		b) 26.7
$N_2PtH(CH_4)$ (**2** or **11**)	19.1	15.7
TS for CH elimination **TS(1-2)** or **TS(10a-11)**	25.7	27.3
TS for CH_4 rotation **TS(2-2)** or **TS(11-11)**	22.1	18.1
N_2PtH (**3** or **12**)	24.5	25.7
N_3PtH (**4** or **13**)	25.1	−28.2
TS for CH_4 loss **TS(2-4)**	31.0	−
$N_2PtH(MeOH)$ (**5** or **14**)	3.7	−6.6
$N_2PtMe(H_2)$ (**15**)	−	22.6
TS for H−H elimination **TS(10a-15)**	−	22.7
N_2PtMe (**6** or **16**)	39.1	36.0
N_3PtMe (**7** or **17**)	40.1	−10.5
$N_2PtMe(MeOH)$ (**8** or **18**)	22.3	9.3
$[(HN{-}N_2)PtMeH_2]^+$ (**19**)	a) −35.4	−
	b) −34.9	
$[N_3PtMeH(H_2)]^+$ (**20**)	−14.2	−
TS for proton shift **TS(19a-20)**	7.1	−
TS for Pt(H2)H isomerization **TS(20-20)**	−14.8	−
$[N_3PtMeH]^+$ (**21**)	−4.6	−
$[N_3Pt(H)_2(CH_4)]^+$ (**22**)	−25.3	−
$[N_3Pt(H)_2]^+$ (**23**)	−18.1	−
$N_3PtMe(H)_2{\cdot}MeOH$ (**24**)	5.4	−
TS for MeOH induced H exchange **TS(24-24)**	49.5	−
$N_3PtMe(H)_2{\cdot}H_2O$ (**25**)	5.0	−
TS for H_2O induced H exchange **TS(25-25)**	51.8	−

this would require two pyrazol rings to be mutually *trans*-oriented, which the rigidity of the system does not allow. The Pt−H bonds are 1.554 Å long, while the Pt−C bond is 2.047 Å long, which agrees well with the value of 2.01(8) Å observed by X-ray crystallography. The Pt−N bond *trans* to the methyl group (2.129 Å) is slightly shorter than the Pt−N bonds *trans* to the hydride ligand (2.146 Å), reflecting the relative *trans* effects of the two ligands. Again, these values compare well with the X-ray bond lengths of 2.20(2) Å, and 2.19(2) and 2.20(2) Å, respectively.[32] It should be noted that the reported crystal structure is not perfectly symmetric, unlike the computed structure. The key calculated and observed bond angles and lengths are listed in Table 2. Overall, there is a good agreement between the two structures.

Platinum−Methane Complex. It has been postulated[32] that the H/D exchange of the methyl protons in **1** proceeds via a methane complex. A number of coordination modes for a σ-methane ligand have been proposed, including η^{1-H}, $\eta^{2-C,H}$, and η^{2-HH} (see Scheme 1, I−III, respectively).[28] For example, in the case of platinum, Heiberg et al.[85] reported that the complex $[(ethylenediamine)Pt(CH_3)(CH_4)]^+$ adopts an $\eta^{2-C,H}$ mode, Siegbahn and Crabtree[21] found an η^{1-H} complex in their investigation of the Shilov reaction, while Bartlett et al.[86] found that $(PH_3)_xPtCl_y(CH_4)$ ($x,y = 0-2$) adopts different binding modes, depending on the exact composition of the complex. There have also been studies on other metal centers, including Ir,[87−90] Rh,[88,89] Co,[89] and Os.[91] In addition, several experimental studies (e.g., refs 31, 33, 38, 83, and 84) support the existence of such a metal−alkane complex.

We searched for all three types of methane complexes but found only one. We were able to identify the complex (η^2-Tp)-PtH($\eta^{2-C,H}$-CH_4) (**2**). The similar Ir(I) complex, $(PH_3)_2Ir(\eta^{2-C,H}$-$CH_3CH_3)(\eta^2$-$CF_3CO_2)$, was found to have the alkane ligand coordinated in the same mode.[90] Complex **2** is at an energy of $\Delta E = 24.1$ kcal/mol relative to **1**. Including thermal and entropic contributions, **2** is at a relative energy of $\Delta G_{298} = 19.1$ kcal/mol. As the platinum center is d^8, one would expect it to be square-planar rather than pentacoordinate, and in fact, we find that the Tp ligand in **2** behaves as a bidentate ligand with one uncoordinated pyrazol ring. It has been shown that the Tp ligand can adopt lower orders of coordination if the situation thus requires.[101] The geometry of **2** is C_1 and the platinum center interacts with a methane C−H bond orientated perpendicular to the square-planar plane with the H pointing away from the noncoordinated pyrazol ring. Table 3 lists the key bond distances in **2**. There clearly is an interaction between the platinum center and one of the methane C−H bonds since one of the C−H bonds in the coordinated methane is considerably longer than the other three (see Table 3: 1.141 Å vs 1.083−1.093 Å). Furthermore, the hydrogen and carbon atoms of the coordinated C−H bond are relatively close to the platinum center yet are much further away than in **1** or compared to the "normal" hydride ligand in this complex. From the different Pt−N bond distances, one can clearly identify the complex as η^2-Tp. This is in agreement with the fact that an 18-electron Pt(II) complex, which would result from η^3-Tp coordination, would be energetically unfavorable due to the high electron density on the metal. One can also see the weak *trans* effect of the methane ligand as compared with that of the hydride or methyl ligands. The nitrogen *trans* to the methane is much closer to the metal center than the one *trans* to the hydride in either **1** or **2** or to the CH_3 ligand in **1**.

To further confirm the structure of **2**, natural bond order (NBO) analyses were carried out on **1** and **2**. The full tables of the Wiberg bond indices for both complexes are included in the Supporting Information. Of special interest is the bonding between the platinum center and the methane unit. In **1**, the Wiberg bond index for the Pt−H bond is 0.66, while for the Pt−C bond it is 0.65. The indices between the platinum center and the methyl hydrogens are 0.01, indicating negligible interactions (Scheme 2). The methyl C−H bond indices are 0.94−0.95, while the bond index between the methyl carbon and the hydride ligand is 0.07. This picture dramatically changes in **2**. The bond index between the platinum center and the hydride is now increased to 0.74. The bond index with the second hydride that is now part of the newly formed methane has decreased significantly to 0.10, and the bond index with the methyl carbon has likewise decreased to 0.15. There is clearly an interaction between the platinum center and the C−H bond in the methane moiety as the bond index with the next closest methyl hydrogen to the platinum center is only 0.02. Within the methane moiety, the agostic C−H bond index is 0.84, while for the other three C−H bonds the indices are 0.92, 0.92, and 0.89.

The bond indices also provide an additional indication on the relative strength of the *trans* effect of the various ligands and on the bidentate nature of the Tp ligand. In **1**, the bond indices of the Pt−N bonds *trans* to the hydride and methyl

(101) Paneque, M.; Sirol, S.; Trujillo, M.; Carmona, E.; Gutiérrez-Puebla, E.; Monge, M. A.; Ruiz, C.; Malbosc, F.; Serra-Le Berre, C.; Kalck, P.; Etienne, M.; Daran, J. C. *Chem. Eur. J.* **2001**, *7*, 3868.

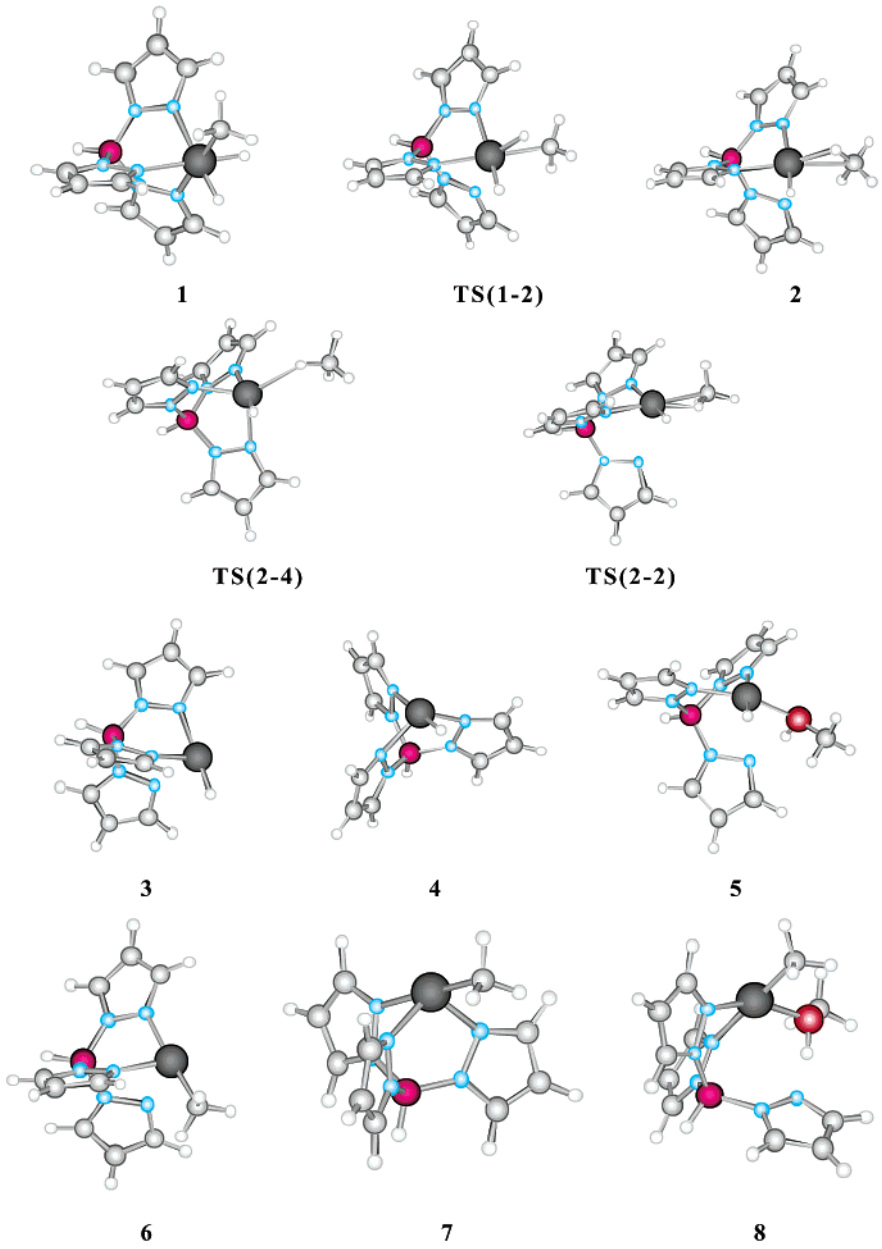

Figure 2. mPW1k/LANL2DZ optimized geometries for the decompostion of $TpPtMe(H)_2$ (**1**). (Color scheme definition: dark gray: Pt; light gray: C; white: H; blue: N; magenta: B; red: O).

ligands are 0.16 and 0.22, respectively. It is known that a hydride has a stronger *trans* effect than a methyl group, and this is reflected in the weaker Pt−N bond *trans* to the hydride. In **2**, the Pt−N bond indices *trans* to the methane moiety and the hydride are 0.50 and 0.19, respectively. It is apparent that the methane ligand has a very weak *trans* effect relative to the hydride. This is in agreement with the above observations on the bond lengths. The bond index of 0.02 between the platinum center and the noncoordinated nitrogen clearly demonstrates that this pyrazol ring is indeed noncoordinated.

Product of Methane Elimination. The product of methane elimination would be TpPtH. This complex can potentially adopt two isomeric structures, one where the Tp ligand is η^2 (**3**) and the other where it is η^3 (**4**). We were able to find minima corresponding to both of these complexes.

The η^2 complex (**3**) is best described as T-shaped. There is very little deviation from the ideal geometry; the two *cis* bond angles, H−Pt−N and N−Pt−N, are 88.8° and 90.0°, respectively, while the *trans* bond angle, H−Pt−N, is 178.6°. The key bond angles and distances are listed in Table 4. This complex has a relative energy of $\Delta E = 37.1$ kcal/mol or $\Delta G_{298} = 24.5$ kcal/mol.

The η^3 complex (**4**) is best described as a "seesaw" or as a drastically distorted square-planar complex. One can view the complex as square-planar where the pair of mutually *trans* pyrazol rings have been bent out of the plane toward each other. Table 4 lists the important bond angles and distances. This complex has a relative energy of $\Delta E = 36.4$ kcal/mol or $\Delta G_{298} = 25.1$ kcal/mol. As this is a d^8 16-electron complex, it would prefer to have an square-planar geometry, yet the rigidity of the Tp ligand does not allow this.

Product of Hydrogen Loss. Aside from methane loss, another potential reaction is the loss of hydrogen (H_2). The product of this reaction would be either (η^2-Tp)PtMe (**6**) or

Table 2. TpPtMe(H)$_2$ Bond Angles (deg) and Lengths (Å) at Various Levels of Theory Compared to the Experimental X-ray Crystallography Structure

angle/bond length	B3LYP/LANL2DZ	mPW1k/LANL2DZ	mPW1k/SDD	mPW1k/LANL2DZ+P	reported structure[a]
			Bond Angles		
C−Pt−N (*trans* to C)	179.4	180.0	179.9	179.8	177
C−Pt−N (*trans* to H)	94.7	94.7	94.6	94.8	91 and 96
N(*trans* to C)-Pt−N(*trans* to H)	84.9	85.3	85.4	85.0	86.8 and 88.1
N(*trans* to H)-Pt−N(*trans* to H)	85.1	84.7	85.5	83.3	84
H−Pt−C	85.7	85.4	85.5	85.5	
H−Pt−H	83.7	83.6	83.4	83.5	
			Bond Lengths		
Pt−H	1.566	1.554	1.545	1.545	not refined
Pt−C	2.075	2.047	2.047	2.030	2.01(8)
Pt−N (*trans* to C)	2.179	2.129	2.132	2.144	2.220(2)
Pt−N (*trans* to H)	2.195	2.146	2.151	2.162	2.19(2) and 2.220(2)
C−H (within methyl)	1.084, 1.097, 1.097	1.086, 1.090, 1.090	1.087, 1.091, 1.091	1.078, 1.091, 1.091	
methyl-C to Pt-hydride distance	2.505	2.469	2.466	2.453	

[a] From ref 32.

Table 3. (η^2-Tp)PtH($\eta^{2-C,H}$-CH$_4$) (**2**) and TS for C−H Reductive Elimination, **TS(1-2)**, Bond Lengths (Å); Geometries Are Optimized at the mPW1k/LANL2DZ Level

bond length	**2**	**TS(1-2)**
Pt−H (hydride)	1.569	1.563
Pt−C	2.400	2.181
Pt−H(CH$_3$)	1.869	1.607
C−H(Pt)	1.141	1.421
C−H (within methyl)	1.083, 1.084, 1.093	1.086, 1.086, 1.088
Pt−N (*trans* to H)	2.166	2.132
Pt−N (*trans* to CH$_4$)	1.972	2.051
Pt−N (noncoordinated)	3.067	2.576

Scheme 2

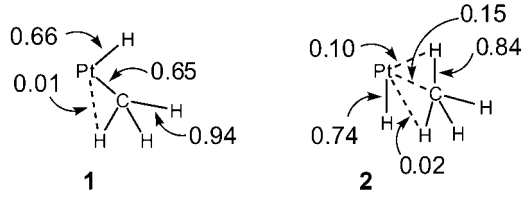

Table 4. (η^2-Tp)PtR (**3**: R = H, **5**: R = Me) and (η^3-Tp)PtR (**4**: R = H, **6**: R = Me) Bond Angles (deg) and Lengths (Å) at the mPW1k/LANL2DZ Level of Theory

bond length/angle	**3** (η^2-Tp), R = H	**4** (η^3-Tp), R = H	**5** (η^2-Tp), R = Me	**6** (η^3-Tp), R = Me
Pt−H	1.572	1.565	2.027	2.023
Pt−N (*cis* to H)	1.953	2.098	2.106	2.121
Pt−N (*trans* to H)	2.117	2.130	1.953	2.098
Pt−N (noncoordinated)	2.828	−	2.930	−
H−Pt−N(*cis*)	88.8	92.8	93.3	94.6
H−Pt−N(*trans*)	178.6	176.7	177.4	179.1
N−Pt−N (*cis*)	90.0	85.4	89.2	84.9
N−Pt−N (*trans*)	−	112.9	−	112.4

(η^3-Tp)PtMe (**7**). These two complexes were also found. Their geometries are similar to those of their hydride analogues **3** and **4**. The former has a relative energy of $\Delta E = 54.0$ kcal/mol or $\Delta G_{298} = 39.1$ kcal/mol while the latter has a relative energy of $\Delta E = 54.7$ kcal/mol or $\Delta G_{298} = 40.9$ kcal/mol. Table 4 lists the key geometric data for these two complexes.

Transition State for the Formation of Methane Complex 2. The transition state, **TS(1-2)**, that corresponds to the C−H reductive elimination and formation of methane was found. The transition state is similar to **1**, but one hydride is bent toward the methyl group forming a C−Pt−H angle of 40.7°. The other C−Pt−H(hydride) angle is 88.2°. One nitrogen has also moved further away from the platinum center. Overall, the bonds are intermediate between **1** and **2**. Table 3 lists the important bond lengths for **TS(1-2)**.

The transition state has an imaginary frequency of 864i cm^{-1}. Animation of the frequency shows that it corresponds to the H moving toward the CH$_3$ group and the corresponding pyrazol ring rotating away from the platinum center. This transition state gives rise to a reaction barrier of $\Delta E^{\ddagger} = 28.5$ kcal/mol or $\Delta G^{\ddagger}_{298} = 25.7$ kcal/mol from **1**, and $\Delta E^{\ddagger} = 7.4$ kcal/mol or $\Delta G^{\ddagger}_{298} = 6.6$ kcal/mol from **2**.

Transition State for Methane Rotation. When **1** is heated in CD$_3$OD, the methyl hydrogens are replaced by deuterium. The initial step, which will be discussed later, is the rapid exchange of the platinum hydrides to produce TpPt(CH$_3$)(D)$_2$. It is reasonable to assume that, subsequently, the methane complex (η^2-Tp)PtH($\eta^{2-C,D}$-DCH$_3$) will be formed, where the C−D bond interacts with the platinum center. If the methane were to rotate, a different C−H bond would interact with the metal. If this were to be followed by the oxidative addition of the C−H bond, via **TS(1-2)**, this would then eventually lead to scrambling of all five hydrogen atoms.

The transition state for this methane rotation, **TS(2-2)**, was found. This transition state is similar to **2**, but the C−H bond that is interacting with the platinum center has rotated by about 90° and is now in the plane, while another C−H bond has come up near the position required for interaction with the metal center. The Pt−C distance has increased slightly from 2.400 to 2.464 Å. There are still no new interactions between the metal center and the methyl group, evident from the three essentially identical C−H bond lengths of 1.082, 1.088, and 1.083 Å, the latter being the C−H bond that will interact with the platinum center. The C−H(Pt) bond is 1.141 Å, identical to that in **2**. **TS(2-2)** has an imaginary frequency of 169i cm^{-1} that corresponds to rotation of the methane group. The rotation of the methane group has a barrier of $\Delta E^{\ddagger} = 2.9$ kcal/mol or $\Delta G^{\ddagger}_{298} = 3.0$ kcal/mol.

Transition State for Methane Loss. A transition state, **TS(2-4)**, for the loss of methane from complex **2** was found. This transition state has an imaginary frequency of 68i cm^{-1} that corresponds to movement of the CH$_4$ toward and away from the platinum center. In the transition state, the Pt−C distance is 3.160 Å, while the closest Pt−H distance is 2.288 Å. Hence, this transition state can be described as an η^{1-H}-methane

Table 5. (η^2-Tp)PtR(MeOH) Complexes (**7** and **8**) Bond Angles (deg) and Lengths (Å) at the mPW1k/LANL2DZ Level of Theory

angle/bond length	**7** (R = H)	**8** (R = Me)
Pt−R	1.576	2.029
Pt−O	2.081	2.089
Pt−N (*trans* to O)	2.081	2.089
Pt−N (*trans* to R)	2.112	2.121
Pt−N (noncoordinated)	3.059	3.073
OH−N	1.744	1.644
O−H	1.012	1.022
N−Pt−N	88.6	87.7
N−Pt−O (*trans*)	159.4	156.8
N−Pt−O (*cis*)	84.0	87.4
N−Pt−R (*trans*)	179.6	179.3
N−Pt−R (*cis*)	91.2	92.7
R−Pt−O	96.1	92.1

structure. The Tp ligand is η^3, suggesting that the transition state connects **2** with **4** rather than **2** with **3**. This transition state on the *E* potential energy surface lies 0.5 kcal/mol below the energy of **3**+CH_4 and 3.5 kcal/mol below **4**+CH_4. This suggests the existence of a **3**···CH_4 or **4**···CH_4 long-range complex, but this complex is of little chemical interest as the loss of methane is very easy due to entropy. Similar complexes have been calculated in the investigation of reductive elimination from $(PH_3)_2Pt(CH_3)H$[86] and in the investigation of the Shilov reaction.[21] On the G_{298} energy surface, there is a barrier for methane loss from **2** of $\Delta G^{\ddagger}_{298} = 11.9$ kcal/mol. For the reverse reaction, methane activation, there is a barrier of $\Delta G^{\ddagger}_{298} = 5.9$ kcal/mol from **4**.

Transition State for Hydrogen Loss. Despite several attempts to find a transition state for the loss of hydrogen from **1**, none could be found. This is not, however, critical as from the energies of the product of hydrogen loss, **6** or **7**, the loss of methane is more favorable, both kinetically and thermodynamically. The energies of **6** and **7** are both significantly higher than the **TS(2-4)**, the highest barrier for methane elimination. Needless to say, they are also higher than the energies of **3** and **4**, the products of methane elimination.

Methanol (Solvent) Complexes. Thus far the solvent has been ignored. Since the reaction is conducted in methanol, it is conceivable that the solvent may coordinate with the complexes. Most of the complexes examined here are either 18-electron Pt(IV) or 16-electron Pt(II) complexes, and therefore, methanol coordination would be energetically unfavorable. Only the η^2-Tp products of methane loss, **3**, and hydrogen loss, **6**, have a vacant site for methanol coordination. Consequently, only the formation of the two complexes, (η^2-Tp)PtR(CH_3OH), R = H (**5**) or R = Me (**8**), would be feasible. These two complexes were found and have relative energies of $\Delta E = 1.1$ kcal/mol or $\Delta G_{298} = 3.7$ kcal/mol for **5**, and $\Delta E = 22.2$ kcal/mol or $\Delta G_{298} = 22.3$ kcal/mol for **8**. While methanol provides a considerable stabilization of the complexes, the high-energy, nonsolvated complexes **3**, **4**, **6**, or **7** first have to be formed. Therefore, complexes **5** and **8** should not affect the kinetics of the reaction. Table 5 contains the key geometric data for these complexes. They are distorted slightly from the square-planar geometry, with the methanol and the *trans*-pyrazol bent out of the plane, as evident from the O−Pt−N bond angle of 159.4° for **5** and 156.8° for **8**. These distortions, however, are significantly smaller than in the η^3-Tp complexes where the corresponding angles are 112.9° (**4**) and 112.4° (**7**). There is also a hydrogen bond formed between the methanol O−H and the noncoordinated pyrazol nitrogen in complexes **5** and **8**.

Overall Reaction Profile. Figure 2 depicts each of the above-mentioned geometries. Figure 3 illustrates the reaction profile based on the above data. It is readily apparent that methane elimination is more favorable than hydrogen elimination.

The key point under investigation is the reason methyl H/D scrambling occurs but methane elimination does not. The reason for this behavior may be deduced from the potential reactions that the methane complex, **2**, can undergo. The three possible reactions are: (1) methane rotation, (2) C−H oxidative addition, and (3) methane loss.

Methane rotation has a low activation barrier and the product of the reaction is **2** but with a different agostic C−H bond. Under the appropriate conditions, the first two reactions can lead to H/D scrambling as described above.

If the barrier for oxidative addition from **2** were higher than the barrier for methane loss, then the complex would lose methane. This is the situation that has been observed for most of the systems reported to date. However, if the reverse were to be true, then one would obtain methyl H/D scrambling without loss of methane. If the two barriers were similar in height, it would be expected that both scrambling and methane loss would be observed leading to various isotopomers of methane. As the difference in barriers increases, then the amount of methane loss would decrease. As we have seen, the barrier for methane loss, **TS(2-4)** is $\Delta G^{\ddagger}_{298} = 11.9$ kcal/mol, while the barrier for C−H oxidative addition, **TS(1-2)**, is $\Delta G^{\ddagger}_{298} = 6.6$ kcal/mol. The significant difference in barrier heights, $\Delta\Delta G^{\ddagger}_{298} = 5.4$ kcal/mol, is the origin of the observed H/D scrambling without concomitant methane loss. Nevertheless, heating of the complex to higher temperatures may lead to methane loss. Indeed, when **1** is heated in benzene at 130 °C for 8 days, one obtains $TpPtPh(H)_2$ and a benzyne complex, ostensibly the products of benzene C−H oxidative addition to either **3** or **4**.[32]

One major question that still remains is the origin of the observed unusual reactivity. One major difference between our system and the others is the nature of the Tp ligand. Most of the other systems involve either mono- or bidentate nitrogen or phosphorus ligands. With the tridentate Tp ligand, the product of methane loss is either **3** or **4**, neither of which is near an ideal square-planar geometry. Complex **3** has 14 electrons and a T-shaped geometry, while **4** has 16 electrons (d^8) with a seesaw geometry. The Tp ligand is too rigid to allow for the ideal η^3 square-planar geometry, thus resulting in the loss of methane to be energetically unfavorable. To test this conjecture, we studied a model system where three monodentate NH_3 ligands replace the tridentate Tp. The results are presented below.

The tris-Ammonia System. Although several analogous systems have been theoretically investigated,[21,85,86,102] none of these investigations utilized the mPW1k functional. Since it is essential to compare energies calculated using the same DFT functional or ab initio method and the same basis set, each intermediate was investigated at the mPW1k/LANL2DZ level with NH_3 ligands replacing the Tp ligand. The energies reported herein are at the mPW1k/LANL2DZ+P//mPW1k/LANL2DZ level. In the Tp system, the borate of the ligand acts as the

(102) Hill, G. S.; Puddephatt, R. J. *Organometallics* **1998**, *17*, 1478.

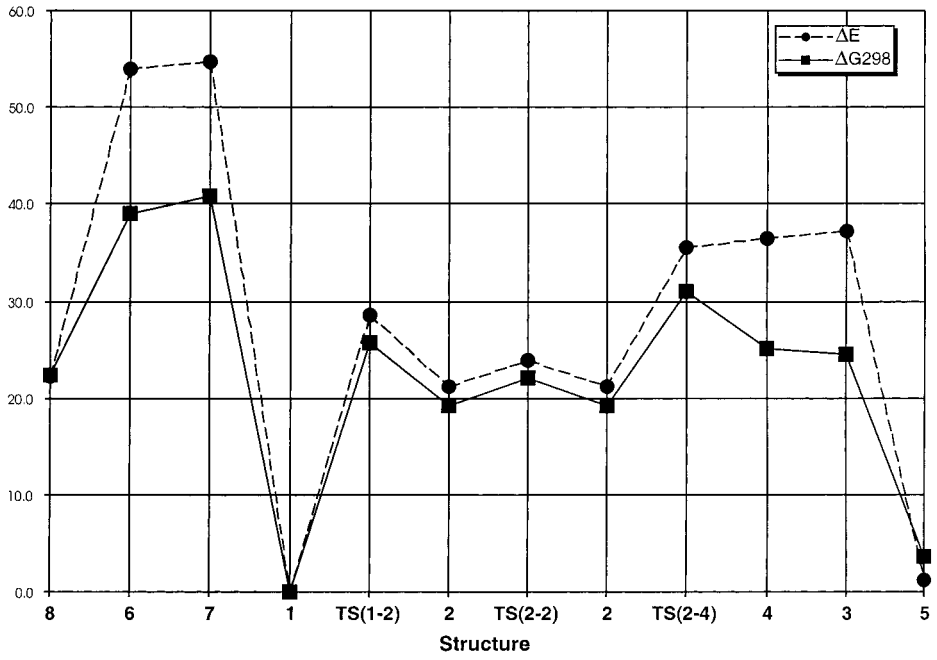

Figure 3. Reaction profile at the mPW1k/LANL2DZ+P//mPW1k/LANL2DZ level of theory for the decomposition of TpPtMe(H)$_2$ (**1**).

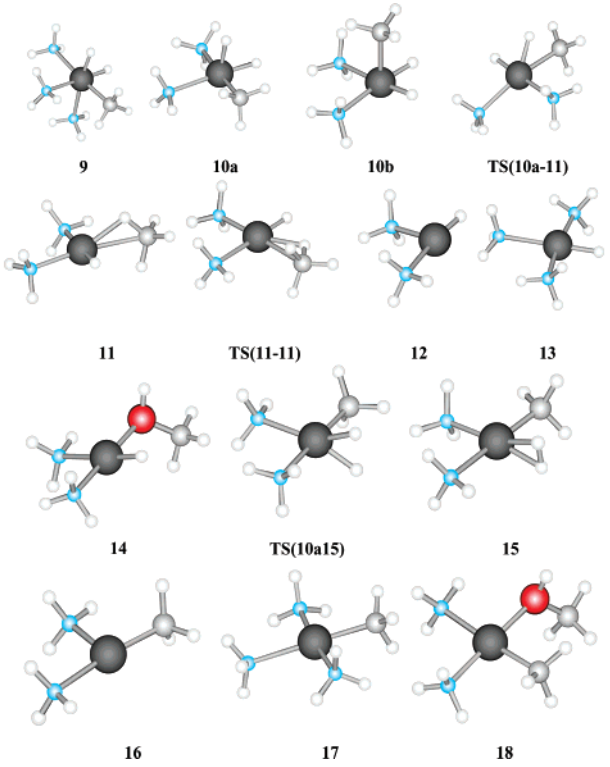

Figure 4. mPW1k/LANL2DZ optimized geometries for the decompostion of [(NH$_3$)$_3$PtMe(H)$_2$]$^+$ (**9**). See Figure 2 for color scheme definition.

counteranion required for overall charge neutrality. In the NH$_3$ system, the complexes being examined are cationic, and it is assumed that there is a noncoordinating, noninteracting outer sphere counteranion that is irrelevant to the calculations. Figure 4 depicts the mPW1k/LANL2DZ optimized geometries of the complexes, while the mPW1k/LANL2DZ+P//mPW1k/LANL2DZ reaction profile is presented in Figure 5. There are some minor differences between the Tp and the tris-NH$_3$ systems. Each step will be discussed briefly below.

The starting complex, [(NH$_3$)$_3$PtMeH$_2$]$^+$ (**9**), is defined as the zero-energy reference. This is an octahedral complex and only the *fac* complex was considered for comparison with the analogous Tp complex **1**. The selected geometric data for this complex are presented in Table 6.

The next step is the loss of an NH$_3$ ligand to give [(NH$_3$)$_2$-PtMe(H)$_2$]$^+$. The analogous Tp complex could not be found. This complex was found to be square pyramidal. Two geometric isomers were found, one where an H is apical (**10a**) and the second where the Me is apical (**10b**). **10a** has a relative energy of $\Delta E = 39.6$ kcal/mol or $\Delta G_{298} = 25.0$ kcal/mol. **10b** has a slightly higher energy at $\Delta E = 40.5$ kcal/mol or $\Delta G_{298} = 26.7$ kcal/mol. This is as one would have expected on the basis of the relative *trans*-effects of the two ligands. Only the lower-energy isomer **10a** will be considered. The ligand dissociation reaction should proceed without a barrier. The important bond angles and distances for **10a** are listed in Table 6.

The next step is the formation of the methane complex, [(NH$_3$)$_2$PtH($\eta^{2-C,H}$-CH$_4$)]$^+$ (**11**). Different methane coordination modes were attempted, but only **11** is a local minimum on the potential energy surface. This complex is similar to its Tp analogue, **2**. It can be described as square-planar with the two NH$_3$ groups arranged in a *cis* arrangement analogous to the Tp ligand. This complex has a relative energy of $\Delta E = 28.3$ kcal/mol or $\Delta G_{298} = 15.7$ kcal/mol. Table 7 lists the key geometric data for **11** as well as for the transition state for reductive elimination, **TS(10a-11)**. As expected, this transition state has the apical hydride bent significantly toward the methyl group. The transition state has an imaginary frequency of 528i cm^{-1} corresponding to C−H reductive elimination. The reaction energy for this step is $\Delta E = -7.6$ kcal/mol or $\Delta G_{298} = -9.6$ kcal/mol. **TS(10a-11)** gives rise to a forward barrier of $\Delta E^{\ddagger} = 2.2$ kcal/mol or $\Delta G^{\ddagger}_{298} = 2.3$ kcal/mol, and a reverse reaction barrier of $\Delta E^{\ddagger} = 13.6$ kcal/mol or $\Delta G^{\ddagger}_{298} = 11.7$ kcal/mol. There is also a transition state for methane rotation, **TS(11-11)**. This transition state has a geometry similar to **TS(2-2)**. The agostic Pt−C−H bond has rotated into the plane

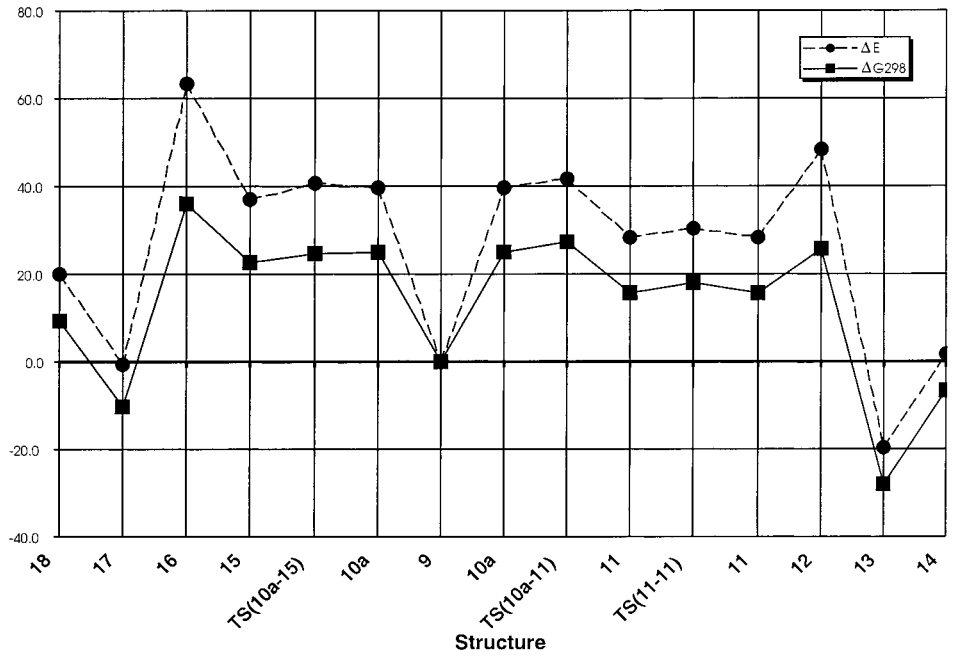

Figure 5. Reaction profile at the mPW1k/LANL2DZ+P//mPW1k/LANL2DZ level of theory for the decompostion of $[(NH_3)_3PtMe(H)_2]^+$ (**9**).

Table 6. Selected mPW1k/LANL2DZ Bond Angles (deg) and Lengths (Å) for **9** and **10a**

bond length/angle	9	10a
Pt−H	1.549, 1.550	1.549 (apical) 1.516 (equatorial)
Pt−C	2.051	2.038
C−H	1.086, 1.087, 1.093	1.084, 1.089, 1.094
C−H (apical)	2.492, 2.501	2.380
H−Pt−H	84.1	76.6
H−Pt−C	86.8, 86.4	82.7 (apical) 87.5 (equatorial)
Pt−N (*trans* to C)	2.223	2.217
Pt−N (*trans* to H)	2.229, 2.230	2.221

of the molecule and another H is moving into position closer to the platinum center to form the new agostic bond. The transition state has an imaginary frequency of 165i cm^{-1} corresponding to the rotation of the methane moiety. There is a barrier for methane rotation of $\Delta E^{\ddagger} = 1.9$ kcal/mol or $\Delta G^{\ddagger}_{298} = 2.4$ kcal/mol. Table 7 also lists selected geometric data for **TS(11-11)**.

The product of methane loss from **11** would be $[(NH_3)_2PtH]^+$ (**12**). This is a T-shaped complex with an NH_3 group situated *trans* to the vacant site. This complex has a relative energy of $\Delta E = 48.3$ kcal/mol or $\Delta G_{298} = 25.7$ kcal/mol. As with the Tp ligand, this 14-electron T-shaped complex is high in energy. A transition state for methane liberation could not be found. The addition of a free NH_3 to **12** yields the 16 electron square-planar complex, $[(NH_3)_3PtH]^+$ (**13**), which is dramatically more stable than **12** with $\Delta E = -19.5$ kcal/mol or $\Delta G_{298} = -28.2$ kcal/mol. Unlike the analogous Tp complex **4**, complex **13** can adopt a nonstrained square-planar geometry. Selected geometric data for complexes **12** and **13** are presented in Table 8. The addition of methanol to **12** instead of NH_3 leads to $[(NH_3)_2PtH(MeOH)]^+$ (**14**), which has a relative energy $\Delta E = 1.7$ kcal/mol or $\Delta G_{298} = -6.6$ kcal/mol. The stabilization afforded by methanol ($\Delta G_{298} = -32.3$ kcal/mol) is less than that provided by NH_3 ($\Delta G_{298} = -53.9$ kcal/mol), in contrast to the Tp situation. The difference in barrier heights for methane loss to produce **13** versus C−H activation to produce **10a** is very small and $\Delta\Delta G^{\ddagger}_{298} = -1.6$ kcal/mol.

Examining the alternative route of hydrogen loss from **9** revealed that, unlike the case of the Tp analogue, an η^2-dihydrogen intermediate was located, $[(NH_3)_2PtMe(\eta^2\text{-}H_2)]^+$ (**15**). This square-planar complex has a relative energy of $\Delta E = 37.1$ kcal/mol or $\Delta G_{298} = 22.6$ kcal/mol. The transition state for H−H reductive elimination, **TS(10a-15)**, was found. For this reaction, a very shallow barrier was found on the E surface. The reaction barrier is $\Delta E^{\ddagger} = 1.0$ kcal/mol and the barrier for the reverse reaction is $\Delta E^{\ddagger} = 3.6$ kcal/mol. Due to the limitations of the rigid rotor-harmonic oscillator approximation used to calculate the thermal corrections, one does not see a reaction barrier on the G_{298} surface and the transition state is 0.3 kcal/mol lower than **10a**. Nonetheless, no chemical significance should be ascribed to this. The transition state has an imaginary frequency of 559i cm^{-1} corresponding to H−H coupling. Table 7 lists the key geometric data for the reaction participants. The change of the Pt−N bond distance *trans* to the hydrogen during this transition is noteworthy. Going from the strong *trans* effect of the hydride ligand to the weak *trans* effect of the dihydrogen ligand, the Pt−N bond decreases in length from 2.221 to 2.058 Å.

The loss of H_2 from **15** generates the expected complex $[(NH_3)_2PtMe]^+$ (**16**), the analogue of **12**. This complex has a relative energy of $\Delta E = 63.2$ kcal/mol or $\Delta G_{298} = 36.0$ kcal/mol. As with the hydride equivalent, this is a T-shaped, 14-electron complex and therefore is high in energy. The loss of H_2 is expected to proceed without a barrier and the reaction has an energy of $\Delta E = 26.1$ kcal/mol or $\Delta G_{298} = 13.4$ kcal/mol. Again, the addition of a free NH_3 ligand gives the stable 16-electron, d^8 square-planar complex, $[(NH_3)_3PtMe]^+$ (**17**), with a relative energy of $\Delta E = -0.6$ kcal/mol or $\Delta G_{298} = -10.5$ kcal/mol. This reaction is also expected to proceed without a barrier and the reaction energy is $\Delta E = -63.7$ kcal/mol or $\Delta G_{298} = -46.5$ kcal/mol. Table 8 lists selected geometric data for these two complexes. Likewise, the addition of methanol to

Table 7. mPW1k/LANL2DZ Bond Angles (deg) and Lengths (Å) for **11**, **15**, **TS(10a-11)**, **TS(10a-15)**, and **TS(11-11)**

angle/bond length	TS(10a-11)	11	TS(11-11)	TS(10a-15)	15
Pt−H	1.552	1.554	1.559	1.567	1.712
Pt−H(CH_3)	1.551	1.872	1.818	–	–
H−H	–	–	–	1.326	0.857
Pt−C	2.112	2.407	2.453	2.040	2.042
C−H(Pt)	1.733	1.140	1.145	–	–
C−H	1.083, 1.086, 1.090	1.083, 1.084, 1.093	1.083, 1.083, 1.089	–	–
Pt−N (*trans* to C)	2.144	2.039	2.037	2.221	2.223
Pt−N (*trans* to H)	2.216	2.217	2.212	2.143	2.058
C−Pt−H(CH_3)	53.9	27.4	26.1	–	–
H−Pt−H	82.9	86.8	70.9	50.0	29.0

Table 8. Selected Bond Angles (deg) and Lengths (Å) for **12**, **13**, **16**, **17** Calculated at the mPW1k/LANL2DZ Level of Theory

angle/bond length	12 (R = H)	13 (R = H)	16 (R = CH_3)	17 (R = CH_3)
Pt−R	1.548	1.562	2.018	2.037
Pt−N (*cis* to R)	2.010	2.066, 2.065	2.014	2.068
Pt−N (*trans* to R)	2.222	2.221	2.225	2.221
R−Pt−N (*cis*)	80.9	86.4, 86.2	86.6	87.4
R−Pt−N (*trans*)	171.5	179.7	171.0	179.5
N−Pt−N (*cis*)	107.6	93.4, 94.1	102.4	92.6
N−Pt−N (*trans*)	–	172.5	–	174.7

16 produces $[(NH_3)_2PtMe(MeOH)]^+$ (**18**), which has a relative energy of $\Delta E = 20.1$ kcal/mol or $\Delta G_{298} = 9.3$ kcal/mol.

From the comparison of the reactivities of **1** and **9**, it is apparent that the origin of the stability of **1** to methane loss is the rigidity of the Tp ligand. The barrier for methane loss from the methane complex, **2,** is higher than the barrier for C−H oxidative addition, and $\Delta\Delta G^{\ddagger}_{298} = 5.4$ kcal/mol. The rigidity of the Tp ligand does not permit it to adopt the *trans* orientation required for the product of methane loss, **4**, and hence precludes the square-planar geometry usually preferred for Pt(II) d^8 complexes. Thus, **4** has a high-energy seesaw geometry, and its formation involves a high barrier of activation. By contrast, in the tris-NH_3 system, the barrier for methane loss from **11** is lower than the barrier for C−H oxidative addition and $\Delta\Delta G^{\ddagger}_{298} = -1.6$ kcal/mol. Not having any difficulty in forming *trans* complexes, **13**, the analogue of **4**, has a nearly ideal square-planar geometry.

H/D Exchange of the Platinum Hydrides. Considering the experimental observation that the H/D exchange of the hydride ligands is faster than the H/D exchange in the methyl group (vide supra), it is clear that the prior exchange of the hydrides cannot involve the methyl group. We examined three potential routes for hydride exchange: (1) direct protonation of **1**, (2) hydrogen bonding with methanol, and (3) hydrogen bonding with water.

The protonation of **1** may involve several alternative sources. Methanol is an unlikely proton source, as its conjugate base, methoxide, is too strong a base. There could, however, be traces of water or acid in the solvent. Reinartz et al.[103] showed experimentally that the complex Tp′PtMe$_2$H (Tp′ = hydridotris(3,5-dimethylpyrazolyl)borate) reacts with acid to yield, as the sole products, methane and $[\{\eta^2$-HPyz′-HB−Pyz′$_2\}$PtMeL$]^+$ (Pyz′=3,5-dimethylpyrazolyl, L = solvent). The elimination of methane in the present case may be prevented by the trace amount of acid or its weaker acidity. Three protonated complexes were identified and are depicted in Figure 6 along with the other related complexes.

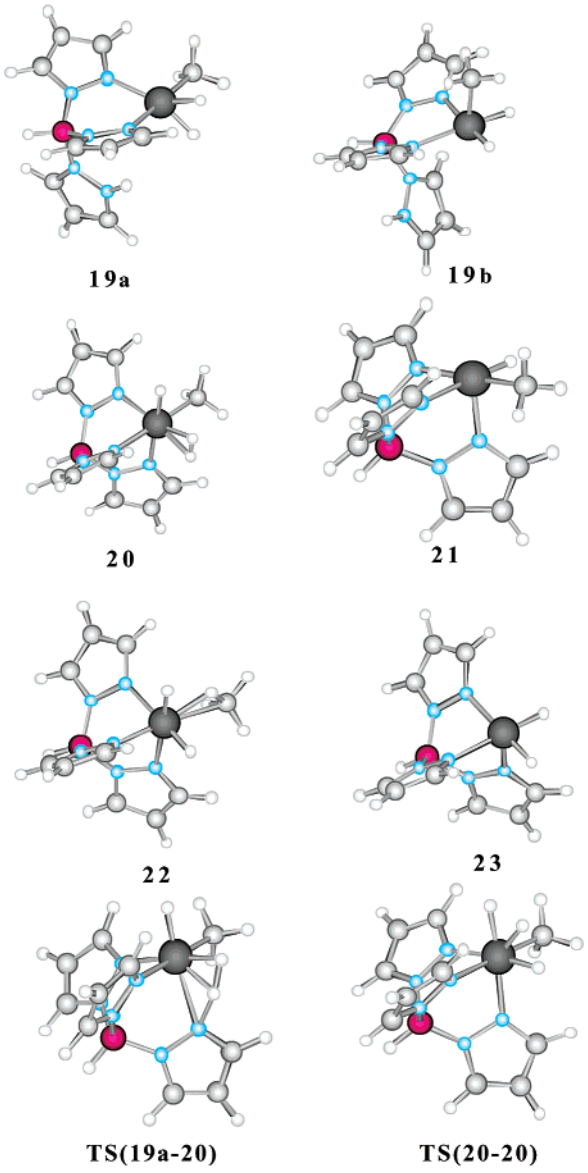

Figure 6. mPW1k/LANL2DZ optimized geometries for the protonation of TpPtMe(H)$_2$ (**1**). See Figure 2 for color scheme definition.

The first is the analogous complex, $[\{\eta^2$-HPyz-HB−Pyz$_2\}$-PtMe(H)$_2]^+$ (**19**, Pyz = pyrazolyl). Two isomers were found for this complex. The lower in ΔG_{298} (**19a**) has a trigonal bipyramidal geometry with axial methyl and pyrazolyl groups. The H−Pt−H angle of 58.8° and the H−H distance of 1.527 Å make this a dihydride complex rather than an η^2-dihydrogen

(103) Reinartz, S.; White, P. S.; Brookhart, M.; Templeton, J. L. *Organometallics* **2000**, *19*, 3854.

complex. The other isomer is at a relative energy (to **19a**) of $\Delta E = 0.0$ kcal/mol or $\Delta G_{298} = 1.4$ kcal/mol, and has a square pyramidal geometry with an apical methyl group. **19a** is the most stable of all the protonated complexes identified.

The second protonated complex is the η^2-dihydrogen complex, $[(\eta^3\text{-Tp})\text{PtMeH}(\text{H}_2)]^+$ (**20**). This complex has an energy relative to **19a** of $\Delta E = 19.0$ kcal/mol or $\Delta G_{298} = 20.6$ kcal/mol. The loss of H_2 from **20** to give $[(\eta^3\text{-Tp})\text{PtMeH}]^+$ (**21**) has a reaction energy of $\Delta E = 8.0$ kcal/mol and $\Delta G_{298} = -4.6$ kcal/mol. The energy of **20** relative to **19a** would give a barrier of suitable height to explain the observed platinum hydride H/D exchange rate. The scrambling can be easily explained by an interchange of the η^2-dihydrogen and the hydride hydrogen atoms. All three atoms are aligned in a row and the scrambling would only involve movement of the middle hydrogen from one outer hydrogen to the other. The corresponding transition state, **TS(20-20)**, an imaginary frequency of 906i cm^{-1} and gives rise to a isomerization barrier of $\Delta E^{\ddagger} = 11.3$ kcal/mol or $\Delta G^{\ddagger}_{298} = 9.5$ kcal/mol. This barrier is small enough to allow for facile scrambling. The transition state connecting these two protonated complexes, **TS(19a-20)**, was likewise found. It corresponds to a concerted reaction with the hydrogen transferring from the pyrazolyl nitrogen to the metal center to form the η^2-dihydrogen ligand while at the same time the third pyrazolyl rotates and binds to the metal center. The transition state has an imaginary frequency of 1479i cm^{-1}, but, unfortunately, the associated barrier of $\Delta E^{\ddagger} = 43.3$ kcal/mol or $\Delta G^{\ddagger}_{298} = 42.4$ kcal/mol is far too high to allow for the reaction to occur.

The third protonated complex is the σ-methane complex, $[(\eta^3\text{-Tp})\text{Pt}(\eta^2\text{-CH}_4)(\text{H})_2]^+$ (**22**). This complex has an energy relative to **19a** of $\Delta E = 7.2$ kcal/mol or $\Delta G_{298} = 9.5$ kcal/mol. The loss of methane from this complex to give $[(\eta^3\text{-Tp})\text{Pt}(\text{H})_2]^+$ (**23**) was determined to be both endothermic and endergonic with $\Delta E = 17.6$ kcal/mol or $\Delta G_{298} = 7.1$ kcal/mol.

The second possibility for the platinum hydride H/D exchange is the involvement of the solvent, CD_3OD. The geometries associated with the last two H/D scrambling routes are shown in Figure 7. Methanol can form hydrogen bonds with **1** to give $\text{TpPtMe}(\text{H})_2\cdot\text{HOCH}_3$ (**24**). The complexation of methanol lowers the energy by $\Delta E = -4.8$ kcal/mol but due to the loss of entropy, $\Delta G_{298} = 5.4$ kcal/mol. A transition state for the methanol induced H/H exchange, **TS(24-24)**, was found. It may be best described as a four-centered concerted transition state. It has an imaginary frequency of 613i cm^{-1}. However, it leads to a barrier of $\Delta E^{\ddagger} = 40.9$ kcal/mol or $\Delta G^{\ddagger}_{298} = 49.5$ kcal/mol. This may be due to the fact that the incoming hydrogen atom enters at an angle to the axial coordination site with an H−Pt−H angle of 39.5°. This distortion from the optimal geometry raises the energy of the transition state to the point that this route seems impossible. In a similar fashion, the exchange could also involve the complexation of a water molecule to give $\text{TpPtMe}(\text{H})_2\cdot\text{H}_2\text{O}$ (**25**), for which $\Delta E = -5.0$ kcal/mol and $\Delta G_{298} = 5.0$ kcal/mol. The barrier for water induced H/H exchange, **TS(25-25)**, is similar to its methanol counterpart. It has an imaginary frequency of 978i cm^{-1} and an H−Pt−H angle of 40.7°. This results in a reaction barrier of $\Delta E^{\ddagger} = 44.8$ kcal/mol or $\Delta G^{\ddagger}_{298} = 51.8$ kcal/mol.

After examining the various possibilities, it is apparent that none of them, while neglecting solvent effects, adequately describe the platinum hydride H/D scrambling. Thus, it is imperative that solvent effects be taken into consideration. A solvent such as methanol or water, which can easily form hydrogen bonds, can greatly assist in hydrogen transfer processes and can stabilize cationic species through solvation. As a first approximation, a single solvent molecule was introduced to assist in proton-transfer processes, such as **TS(19a-20)**. Despite several attempts at several different proton transfer reactions, using both water and methanol as the transfer assisting molecule, no reasonable structure could be obtained. We have therefore concluded that bulk solvent effects cannot be neglected in the investigation of the platinum hydride H/D exchange where it appears that the solvent plays a key role in the process. Nevertheless, properly including solvent effects in our calculations is far beyond both the scope of the investigation and the computational resources available to us at this time. Of the various possibilities presented here, we believe that the most plausible exchange involves the solvent in a four-centered concerted transition state akin to **TS(24-24)** or **TS(25-25)**. Such a transition state would be stabilized by the inclusion of solvent effects and this would thus lower the barrier of H/D exchange. An additional plausible exchange pathway would involve a four-centered $\text{MH}^{\delta-}\cdots\text{H}^{\delta+}\text{OR}$ mechanism similar to that proposed by Koelliker and Milstein for Ir.[104] Unfortunately, we cannot at this time substantiate this claim nor determine exactly how the various intermediates and transition states appear.

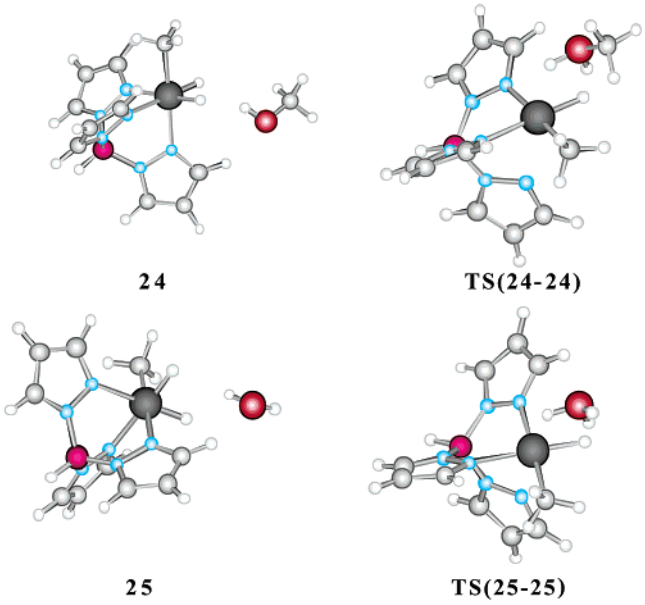

Figure 7. mPW1k/LANL2DZ optimized geometries for the solvent-assisted exchange of the metal hydrides in $\text{TpPtMe}(\text{H})_2$ (**1**). See Figure 2 for color scheme definition.

α-Hydride Elimination Route. An alternate route to the platinum−methane route considered thus far is the α-hydride elimination route. This route is in essence the opposite of the other, in that a hydrogen is transferred from the methyl ligand rather than to it. The product of the reaction would be a carbene complex.

We attempted to find the complex $(\eta^2\text{-Tp})\text{Pt}(\text{CH}_2)(\text{H})_3$. All attempts led back to the starting complex **1**. Nevertheless, we were able to locate the complex *cis,cis*-$[\{\eta^2\text{-HPyz-HB−Pyz}_2\}\text{-Pt}(\text{CH}_2)(\text{H})_2]$ (**26**). In this complex, a hydrogen has been

(104) Koelliker, R.; Milstein, D. *J. Am. Chem. Soc.* **1991**, *113*, 8524.

Table 9. Reaction Profile and Comparison of $\Delta\Delta G^{\ddagger}_{298}$ (see text) at Various Levels of Theory

	optimized at B3LYP/LANL2DZ		optimized at mPW1k/LANL2DZ		optimized at mPW1k/SDD		
energy at	B3LYP/ LANL2DZ	B3LYP/ LANL2DZ+P	mPW1k/ LANL2DZ	mPW1k/ LANL2DZ+P	mPW1k/ SDD	mPW1k/ SDB-cc-pVDZ	mPW1k/ SDB-cc-pVTZ
8	15.3	19.6	17.7	22.3	22.5	26.1	27.5
6	36.9	35.7	40.7	39.1	–	–	–
7	36.6	37.4	40.1	40.8	43.8	46.7	44.9
1	0.0	0.0	0.0	0.0	0.0	0.0	0.0
TS(1-2)	25.3	24.2	27.3	25.7	29.1	24.8	24.2
2	19.2	18.2	20.7	19.1	23.8	21.0	19.3
TS(2-2)	21.8	20.8	23.7	22.1	26.9	24.2	22.2
2	19.2	18.2	20.7	19.1	23.8	21.0	19.3
TS(2-4)	26.1	27.3	29.7	31.0	32.5	34.6	34.2
4	20.1	21.7	23.5	25.1	26.3	29.1	27.9
3	21.4	21.1	25.1	24.5	–	–	–
5	−2.6	2.0	−0.9	3.7	3.0	6.1	7.9
$\Delta\Delta G^{\ddagger}_{298}$	0.8	3.1	2.4	5.4	3.4	9.8	10.1

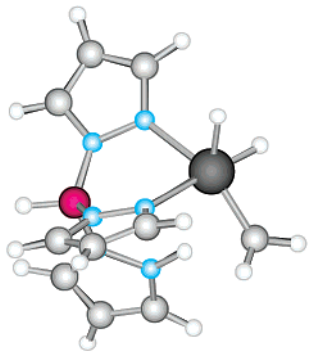

26

Figure 8. mPW1k/LANL2DZ optimized geometry of *cis,cis*({η_2-HPyz-HB−Pyz$_2$}Pt(CH$_2$)(H)$_2$ (**26**), the intermediate in the α-hydride elimiation route. See Figure 2 for color scheme definition.

abstracted by one of the pyrazolyl bases of the Tp ligand. This is a slightly distorted square pyramidal complex with an apical hydride. The carbene is orientated parallel to the basal plane. This complex is depicted in Figure 8. This intermediate can be viewed as the product of α-hydrogen elimination followed by proton abstraction from the metal center by a base, specifically the pyrazolyl ring of the Tp ligand. This complex lies at such a high energy (ΔE = 71.1 kcal/mol or ΔG_{298} = 69.0 kcal/mol) that one can readily discount this route as a potential reaction pathway.

Method Comparison. The thermal decomposition of **1** was examined at levels of theory other than the above-described mPW1k/LANL2DZ+P//mPW1k/LANL2DZ level. Specifically, we used:

(1) mPW1k/LANL2DZ

(2) mPW1k/LANL2DZ+P//mPW1k/LANL2DZ

(3) mPW1k/SDD

(4) mPW1k/SDB-cc-pVDZ//mPW1k/SDD

(5) mPW1k/SDB-cc-pVTZ//mPW1k/SDD

(6) B3LYP/LANL2DZ

(7) B3LYP/LANL2DZ+P

See Computational Details section for a brief explanation of each exchange-correlation functional and basis set. Table 9 presents the reaction profile for the various levels of theory. From these calculations, several observations were made. First of all, the η^2 complexes **3** and **6** could not be found using the SDD basis set. The attempts to find them consistently yielded the η^3 complexes **4** and **7**.

It was also observed that the mPW1k DFT functional yielded higher barriers than B3LYP. It has previously been observed that B3LYP tends to underestimate barrier heights,[63,64,105] and it would appear that mPW1k tends to partially correct this. This in not too surprising, since mPW1k, unlike most other functionals, was parametrized using barrier heights and reaction energies.[62] In one test of 22 reactions using a large basis set, it was shown that the mean signed error for mPW1k is −1.0 kcal/mol, while for B3LYP it is −3.5 kcal/mol.[63] In our investigation, the main objective is, in essence, to determine $\Delta\Delta G^{\ddagger}_{298}$ (vide supra). For this value to have any meaning, it is imperative that the errors be reduced as much as possible. Table 9 lists the value of $\Delta\Delta G^{\ddagger}_{298}$ at the various levels. It is readily obvious that the B3LYP functional does not perform as well as the mPW1k functional. In fact, at the B3LYP/LANL2DZ level, which can be described as the most widely used level of theory, the two barriers are nearly equal in height. If one were to rely on the B3LYP functional, one would erroneously conclude that methane liberation may indeed occur.

Furthermore, one can clearly see the importance of using a sufficiently large basis set. While the errors involved is using the LANL2DZ basis set rather than the LANL2DZ+P basis set, or the SDD rather than SDB-cc-pVDZ basis set, are small, they are neither systematic nor negligible. In regard to $\Delta\Delta G^{\ddagger}_{298}$ in Table 9, we note that the mPW1k/SDB-cc-pVDZ//mPW1k/SDD result, 9.8 kcal/mol, is still significantly higher than its mPW1k/LANL2DZ+P//mPW1k/LANL2DZ counterpart of 5.4 kcal/mol. This is despite the fact that the two basis sets are fundamentally similar in size and differ primarily in the RECP used on the metal. Furthermore, the energy calculations with the SDB-cc-pVTZ basis set yield a value for $\Delta\Delta G^{\ddagger}_{298}$ of 10.1 kcal/mol that is extremely close to the SDB-cc-pVDZ basis set result, and one can assume that the latter is sufficiently large to yield meaningful results. Apparently, the exceedingly time-consuming SDB-cc-pVTZ calculations do not significantly alter our conclusions and we can assume our results to be converged in terms of the basis set. It goes without saying that the large size of the system (over 30 atoms) precludes comparing the results with correlated ab initio calculations in a meaningfully large basis set, such as, CCSD(T)/SDB-cc-pVTZ.

(105) Durant, J. L. *Chem. Phys. Lett.* **1996**, *256*, 595.

From the above, one can conclude that the commonly used B3LYP/LANL2DZ combination performs unsatisfactorily in predicting reaction profiles. Rather, it is recommended that the newer mPW1k functional be used in conjunction with a larger basis set. From the above results, it would seem that the mPW1k/SDB-cc-pVDZ//mPW1k/SDD level of theory is the method of choice for investigating reactions, especially where accurate barrier heights are of importance.

Conclusions

We have reported on the kinetic stability of the complex $TpPtMe(H)_2$ (**1**), which upon heating in methanol does not eliminate methane. On the other hand, when deuterated methanol is used, the hydrides and the methyl hydrogens are all reversibly replaced by deuterium. The remarkable stability of this complex can be explained by the rigidity of the Tp ligand, which does not allow the square-planar geometry required for the product of methane (or hydrogen) elimination. The kinetic results demonstrate the existence of a σ-methane complex, a proposed key intermediate in reductive elimination (C−H coupling) reactions. From a computational standpoint, the relative barrier heights of H/D scrambling and methane liberation are quite sensitive to both the basis set and the choice of exchange-correlation functional. The use of the commonly applied unpolarized LANL2DZ or SDD basis set-RECP combinations, as well as exchange-correlation functionals not adapted to transition states, will lead to qualitatively incorrect chemistry.

Acknowledgment. Research at the Weizmann Institute was supported by the Helen and Martin Kimmel Center for Molecular Design and by the *Tashtiyot* (Infrastructures) program of the Ministry of Science and Technology (Israel) as well as by a computer time grant from the (Israel) Inter-University Computing Center. M.A.I. acknowledges a Doctoral Fellowship from the Feinberg Graduate School (Weizmann Institute of Science). H.C.L. and E.K. acknowledge the Skaggs Institute for Chemical Biology for a fellowship and financial support, respectively.

Supporting Information Available: Complete crystallographic data for **1** and all the calculated structures of complexes **1**−**26** along with the connecting transition states (in Xmol (.xyz) format) in PDF format. This material is available free of charge via the Internet at http://pubs.acs.org. The calculated structures can also be found on the Internet at the Uniform Resource Locator (URL) http://theochem.weizmann.ac.il/web/papers/Pt-CH4.html.

JA025667V